Integral Geometry and General Adaptive Neighborhoods for Multiscale Image Analysis

Séverine Rivollier, Johan Debayle, Jean-Charles Pinoli

Integral Geometry
and General Adaptive Neighborhoods
for Multiscale Image Analysis

Séverine Rivollier, Johan Debayle, Jean-Charles Pinoli

Ecole Nationale Supérieure des Mines de Saint-Etienne
CIS - LPMG, UMR CNRS 5148
158 cours Fauriel, 42023 Saint-Etienne cedex 2, France
tel: +33 477 420 219 / fax: +33 477 499 694
e-mail: rivollier@emse.fr, debayle@emse.fr, pinoli@emse.fr

Abstract: In quantitative image analysis, Minkowski functionals are becoming standard parameters for topological and geometrical measurements. Nevertheless, they are limited to binary images or to sections of gray-tone images and are achieved in a global and monoscale way. The use of General Adaptive Neighborhoods (GANs) enables to overcome these limitations. The GANs are spatial neighborhoods defined around each point of the spatial support of a gray-tone image, according to three (GAN) axiomatic criteria: a criterion function (luminance, contrast, . . .), an homogeneity tolerance with respect to this criterion, and an algebraic model for the image space. Thus, the GANs are simultaneously adaptive with the analyzing scales, the spatial structures and the image intensities.

This paper aims to introduce the GAN-based Minkowski functionals, which allow a gray-tone image analysis to be realized in a local, adaptive and multiscale way. The Minkowski functionals are computed on the GAN of each point of the spatial support of a gray-tone image, enabling to define the so-called Minkowski maps by assigning the Minkowski functional value to each point. The histograms of these maps provide a statistical distribution of the topology and geometry of the gray-tone image structures, and not only of the image intensities. The impact of the GAN characteristics, as well as the impact of multiscale transformations, are analyzed in a qualitative global and local way through these GAN-based Minkowski maps and histograms. This multiscale image analysis is illustrated on the test image 'Lena' and also applied in both the biomedical and materials areas.

Keywords: GAN-based Minkowski maps and histograms, General Adative Neighborhoods, Integral Geometry, Minkowski functionals, Multiscale image analysis

NOMENCLATURE

This section presents a list of all the used symboles and their meaning.

A	area
P	perimeter
χ	Euler number
A_A	specific area
P_A	specific perimeter
χ_A	specific Euler number
μ	specific Minkowski functional
GLIP	General Linear Image Processing
$\bigcirc$	GLIP framework
$\oplus$	vector addition of the GLIP framework
$\ominus$	vector subtraction of the GLIP framework
$\otimes$	scalar multiplication of the GLIP framework
CLIP	Classical Linear Image Processing
$+$	vector addition of the CLIP framework
$-$	vector subtraction of the CLIP framework
$\times$	scalar multiplication of the CLIP framework
LIP	Logarithmic Image Processing
$\triangle$	LIP framework
$\boxplus$	vector addition of the LIP framework
$\triangle\!\!\!-$	vector subtraction of the LIP framework
$\triangle\!\!\!\times$	scalar multiplication of the LIP framework
$\mathcal{I}$	space of gray-tone images
$\mathcal{C}$	space of analyzing criteria
$\mathbb{E}_{\bigcirc}$	intensity value range
D	image spatial support
f	gray-tone image
h	analyzing criterion
$m_{\bigcirc}$	homogeneity tolerance
$V_{m_{\bigcirc}}^{h}(x)$	GAN of $x \in D$
$\mu_{m_{\bigcirc}}^{h}$	GAN-based Minkowski map

$$\mathrm{H}\left(\mu_{m_{\bigcirc}}^{h}\right) \qquad \text{histogram of the}$$

GAN-based Minkowski map

$\mu_{\bigcirc}^{f}(.)$ GAN-based Minkowski function
according to the homogeneity tolerance $m_{\bigcirc}$

$\mu_{m_{\bigcirc}}^{T(f)}(.)$ GAN-based Minkowski function
according to the radius of the structuring element
used for a morphological transformation T

1. INTRODUCTION

This paper aims to introduce a novel approach for analyzing gray-tone images in a local, adaptive and multiscale way. A segmentation process, generally used before quantitative image analysis, is not here required. The quantitative description is directly applied on the raw gray-tone images. Geometrical and topological measurements, through Minkowski functionals, see Michielsen and De Raedt (2001), are performed on spatial neighborhoods associated to each point of the gray-tone image support. These specific neighborhoods, named General Adaptive Neighborhoods (GANs), see Debayle and Pinoli (2005, 2006), are simultaneously adaptive with the spatial structures, the image intensities and the analyzing scales. They are based on three axiomatic criteria: an analyzing criterion, an homogeneity tolerance and an algebraic model. These GAN enable to define the so-called GAN-based Minkowski maps which assign a measurement (based on the local Minkowski functionals) to each point of the spatial support of the gray-tone image to be studied.

First, the second and third sections recall the notions of Minkowski functionals and of general adaptive neighborhoods, respectively. Then, the fourth and fifth sections introduce the GAN-based Minkowski maps and histograms and illustrate them for various analyzing critera and algebraic models. Thereafter, the impact of the homogeneity tolerance and of a multiscale transformation are analyzed through these GAN-based Minkowski maps. This multiscale image analysis is illustrated on the test image 'Lena' and also applied in both the biomedical and materials areas.

2. MINKOWSKI FUNCTIONALS AND DENSITIES

In quantitative image analysis, Minkowski functionals, see Minkowski (1903), are becoming standard parameters for topological and geometrical measurements, see Coster and Chermant (1985) and Michielsen and De Raedt (2001). A description of the shape of a two-dimensional spatial pattern is provided, using the three 2D Minkowski functionals (up to a constant): area, perimeter, and Euler number, denoted A, P and χ, respectively.

These functionals are defined on the class of nonempty compact convex sets (convex bodies) of $\mathbb{R}^2$, and satisfy five properties (increasing, invariance under rigid motions, homogeneity, additivity, continuity vs. the Hausdorff metric). They have been extended (excluding the properties of increasing and continuity) to the convex ring, see Mecke and Stoyan (2000), i.e. the set of all finite unions of convex bodies of $\mathbb{R}^2$, which may be considered as a realistic Euclidean model for digital planar images.

In this paper, the densities instead of the intensities of these functionals, i.e. the ratio of the Minkowski intensity functionals by the area of the spatial support, will be used. These Minkowski density functionals are called the specific area, the specific perimeter, and the specific Euler number, and are denoted, A_A, P_A and χ_A, respectively.

3. GENERAL ADAPTIVE NEIGHBORHOODS

The GANIP (General Adaptive Neighborhood Image Processing) approach, see Debayle and Pinoli (2005, 2006, 2009), provides a general framework for multiscale, local and adaptive processing and analysis of gray-tone images.

It is based on an image representation by means of specific spatial neighborhoods, named General Adaptive Neighborhoods (GANs). Indeed, GANs are simultaneously adaptive with:

- the spatial structures: the size and the shape of the neighborhoods are adapted to the local context of the image,
- the analyzing scales: the scales are given by the image itself, and not *a priori* fixed,
- the intensity values: the neighborhoods are defined according to the GLIP (General Linear Image Processing) algebraic mathematical framework, see Oppenheim (1967) and Pinoli (1997), enabling to involve the physical and/or psychophysical image formation laws.

For a gray-tone image f, a GAN of a point x belonging to the spatial support $D \subseteq \mathbb{R}^2$, denoted $V_{m_{\bigcirc}}^{h}(x)$, is a connected subset of D. It is homogeneous with respect to an analyzing criterion h (such as luminance, contrast, thickness, . . .) using an homogeneity tolerance, denoted $m_{\bigcirc}$. The symbol $\bigcirc$ stands for the algebraic model for the space of gray-tone images. The space of gray-tone images (resp. analyzing criteria), defined on the spatial support and valued in a real number interval $\tilde{\mathbb{E}}$ (resp. $\mathbb{E}_{\bigcirc}$) is denoted $\mathcal{I}$ (resp. $\mathcal{C}$). The homogeneity tolerance $m_{\bigcirc}$ belongs to the positive intensity value range $\mathbb{E}_{\oplus} := \{t \in \mathbb{E}_{\bigcirc} | t \geq 0_{\bigcirc}\}$, where $0_{\bigcirc}$ denotes the neutral element for vector addition, see Debayle and Pinoli (2006). The GAN of a point x is mathematically defined as follows:

$$V_{m_{\bigcirc}}^{h}(x) := C_{h^{-1}([h(x) \ominus m_{\bigcirc}; h(x) \oplus m_{\bigcirc}])}(x) \qquad (1)$$

where $C_X(x)$ denotes the path-connected component (with the usual Euclidean topology on D) of $X \subseteq D$ holding x. The criterion function h is represented in a GLIP (General Linear Image Processing) model, see Oppenheim (1967) and Pinoli (1997), i.e. a vector space with its vector addition $\oplus$ and its scalar multiplication $\otimes$.

For instance, the operations $\oplus$ and $\otimes$ of the usual CLIP (Classical Linear Image Processing) framework correspond to the usual operations between images, $+$ and $\times$ respectively. The vector addition and subtraction and the scalar multiplication of the LIP (Logarithmic Image Processing) framework, see Jourlin and Pinoli (1988, 2001), denoted $\triangle\!\!\!\!\!\bigtriangleup$, $\triangle\!\!\!\!\!\bigtriangleup$ and $\triangle\!\!\!\!\!\bigtriangleup$ respectively, are defined as follows:

$$f \,\triangle\!\!\!\!\!\bigtriangleup\, g = f + g - \frac{fg}{M} \qquad (2)$$

$$f \triangle g = M \left(\frac{f - g}{M - g} \right) \qquad (3)$$

$$\alpha \triangle f = M - M \left(\frac{M - f}{M} \right)^{\alpha} \qquad (4)$$

where f and g are gray-tone images, $\alpha \in \mathbb{R}$ is a scalar, and $M \in \mathbb{R}_+$ denotes the upper bound of the range where intensity images are valued. The LIP framework has been proved to be consistent with the transmittance and the multiplicative reflectance/transmittance image formation model, and with several laws and characteristics of human brightness perception, see Pinoli (1997). The GANIP approach in the special case where the LIP framework is used has been studied and applied in Pinoli (2007).

The GAN satisfy several properties as stated in the following (proved in Debayle and Pinoli (2006)). For all $(h, m_\bigcirc, m_\bigcirc^1, m_\bigcirc^2, x, x_1, x_2) \in \mathcal{C} \times (\mathbb{E}_\oplus)^3 \times D^3$,

- reflexivity:

$$x \in V_{m_\bigcirc}^h(x) \qquad (5)$$

- increasing with respect to $m_\bigcirc$:

$$m_\bigcirc^1 \leq m_\bigcirc^2 \Rightarrow V_{m_\bigcirc^1}^h(x) \subseteq V_{m_\bigcirc^2}^h(x) \qquad (6)$$

- equality between iso-valued points:

$$\begin{pmatrix} x_1 \in V_{m_\bigcirc}^h(x_2) \\ h(x_1) = h(x_2) \end{pmatrix} \Rightarrow V_{m_\bigcirc}^h(x_1) = V_{m_\bigcirc}^h(x_2) \qquad (7)$$

- $\oplus$-translation invariance:

$$\forall c_\bigcirc \in \mathbb{E}_\bigcirc : V_{m_\bigcirc}^{h \oplus c_\bigcirc}(x) = V_{m_\bigcirc}^h(x) \qquad (8)$$

- $\otimes$-multiplication compatibility:

$$\forall \alpha \in \mathbb{R}_+^* : V_{m_\bigcirc}^{\alpha \otimes h}(x) = V_{\frac{1}{\alpha} \otimes m_\bigcirc}^h(x) \qquad (9)$$

Figure 1 gives a visual impression, on a 1D example, of the computation of a GAN in the LIP framework (i.e. with the $\triangle$ vector addition (Eq. 2) and the $\triangle$ vector subtraction (Eq. 3)).

Figure 2 illustrates the GANs of two points computed with the luminance criterion in the CLIP (Classical Linear Image Processing) framework (the operations $\oplus$ and $\otimes$ correspond to the usual operations between images, $+$ and $\times$ respectively) on a human retina image.

The General Adaptive Neighborhoods are intrinsically defined by the local image structures. Thus, the GANs $\{V_{m_\bigcirc}^h(.)\}_{m_\bigcirc}$ allow a new multiscale representation of gray-tone images to be defined.

Defined on the spatial support D of an image (Fig. 3), the GANs are simultaneously adaptive with the spatial structures, the analyzing scales and the intensity values. On the contrary, the shape and size of the classical neighborhoods $\{B_r(.)\}_r$ (centered homothetic isotropic discs of radius r), generally used as analyzing windows for image transforms, are *a priori* fixed.

4. GAN-BASED MINKOWSKI MAPS

This novel multiscale representation of gray-tone images enables to define GANs measurements, allowing a gray-tone image quantitative analysis, in a local, adaptive and
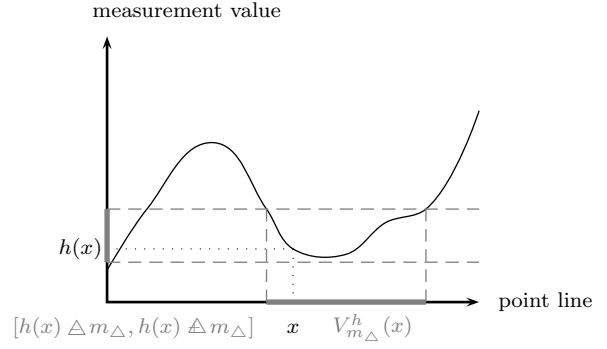

Fig. 1. One-dimensional computation of a GAN set $V_{m_\triangle}^h(x)$ in the LIP framework. For a point x, a range of tolerance $m_\triangle$ is first computed around $h(x)$. Secondly, the inverse mapping of this interval gives a subset of the 1D spatial support. Finally, the path-connected component holding x provides the GAN $V_{m_\triangle}^h(x)$.

(a) original retina image with two (white) points x and y

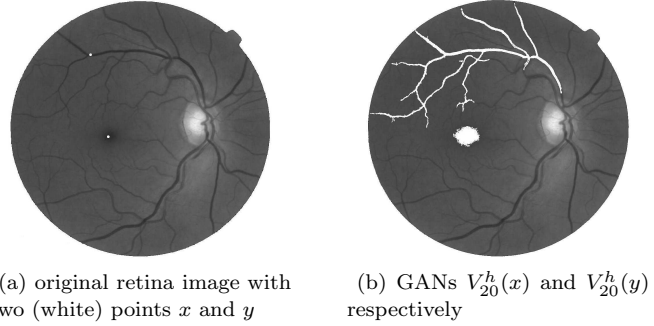(b) GANs $V_{20}^h(x)$ and $V_{20}^h(y)$ respectively

Fig. 2. The GANs of the two points x and y of the original image (a) are connected and homogeneous (b) with respect to the luminance criterion using the tolerance value $m = 20$ within the CLIP framework. The GANs are adapted to the image structures.
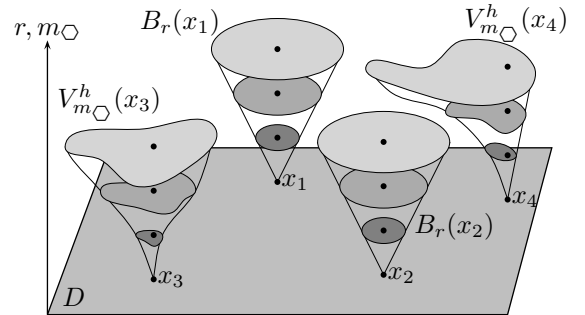

Fig. 3. Example of adaptive $V_{m_\bigcirc}^h$ and non-adaptive B_r analyzing windows with three values both for the homogeneity tolerance parameter $m_\bigcirc$, and for the disks radius r. The shape of $B_r(x_1)$ and $B_r(x_2)$ are identical and $\{B_r(x)\}_r$ is a family of homothetic sets for each point $x \in D$. On the contrary, the shapes of $V_{m_\bigcirc}^h(x_3)$ and $V_{m_\bigcirc}^h(x_4)$ are dissimilar and $\{V_{m_\bigcirc}^h(x)\}_{m_\bigcirc}$ is not a family of homothetic sets.

multiscale way. Indeed, for each point x of the gray-tone image f, various measurements, such as area, orientation, concavities number, ... see Coster and Chermant (1985) and Rivollier (2006), of the GAN $V_{m_\bigcirc}^h(x)$, can be computed.

In this paper, the considered measurements are the Minkowski density functionals. These functionals can be estimated in an efficient way, see Nagel (1999) and Osher and Mücklich (2001).

4.1 Definition

A GAN-based Minkowski map is defined by assigning a value for each point x which represents a GAN Minkowski density functional of $V_{m_\bigcirc}^h(x)$. In a more explicit way, the GAN-based Minkowski map $\mu_{m_\bigcirc}^h$ of a gray-tone image f with respect to the Minkowski density functional μ (area: $\mu \equiv A_A$, perimeter: $\mu \equiv P_A$, Euler number: $\mu \equiv \chi_A$) is defined by:

$$\mu_{m_\bigcirc}^h : \begin{cases} D \to & \mathbb{R} \\ x \mapsto \mu\left(V_{m_\bigcirc}^h(x)\right) \end{cases} \tag{10}$$

where $V_{m_\bigcirc}^h(x)$ is the GAN of the point x with respect to the analyzing criterion h using the homogeneity tolerance $m_\bigcirc$ in a GLIP framework.

Figure 4 illustrates some GAN-based Minkowski maps of the image 'Lena' f. The GANs are homogeneous with respect to the luminance criterion $(h \equiv f)$ using the tolerance value $m = 40$ in the context of the CLIP framework. Therefore, the value $\mu_{m_\bigcirc}^h(x)$ of each point x of the Minkowski map corresponds to the density μ of the GAN $V_{40}^f(x)$. The GANs depend on three axiomatic criteria (Eq. 1): an analyzing criterion, an algebraic GLIP model for the criterion mapping space, and an homogeneity tolerance with respect to this criterion. The two following subsections show, from a visual point of view, the impact of the two firsts characteristics on the Minkowski maps (Eq. 10). The impact of the homogeneity tolerance will be studied in the next section.

4.2 Impact of the analyzing criterion

The GANs are homogeneous with respect to a criterion function h (such as luminance, contrast, thickness, ...). For instance, the luminance criterion is defined by $h \equiv f$ where f is the original gray-tone image. A contrast criterion can also be used. For instance, the contrast image, denoted c, associated to the gray-tone image, can be defined in a discrete way in the context of the CLIP framework as:

$$c : \begin{cases} D \to \mathbb{R}_+ \\ x \mapsto \dfrac{1}{\#N(x)} \sum_{y \in N(x)} |f(x) - f(y)| \end{cases} \tag{11}$$

where $N(x)$ is a neighborhood of the point x (for instance, points in the window 3×3 centered on x).

Figure 5 illustrates the GAN-based Minkowski maps of a fibronectin image f with respect to the luminance criterion

f and the contrast criterion c using the homogeneity tolerance $m = 20$ in the context of the CLIP framework. The results show that the extracted zones are not the same for the two criteria.

4.3 Impact of the mathematical framework

Figure 6 illustrates the GAN-based Minkowski maps of a zinc sulfide image f acquired by scanning electron microscopy imaging with respect to the luminance criterion f using the homogeneity tolerance value 50 in the context of the CLIP and LIP mathematical frameworks, respectively.
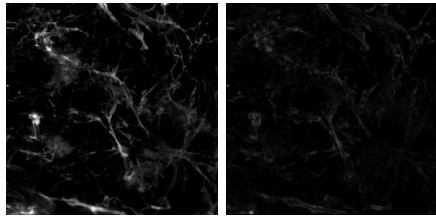
These GAN-based Minkowski maps can be used for image segmentation. A usual intensity thresholding does not always extract the desired structures of a gray-tone image. Using appropriate GAN axiomatic criteria (analyzing criterion, mathematical framework, homogeneity tolerance), the GAN-based Minkowski maps highlight these structures and the desired segmentation is obtained by thresholding these GAN-based Minkowski maps.

The next section focuses on the histograms of these GAN-based Minkowski maps.
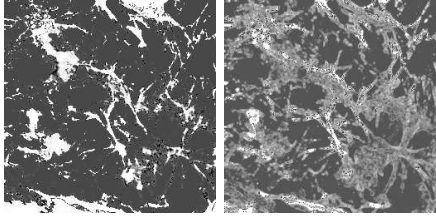

(a) original image f

(b) $(\chi_A)_{40}^f$ (c) $(P_A)_{40}^f$ (d) $(A_A)_{40}^f$

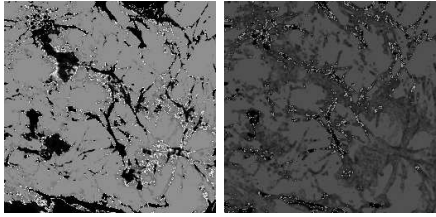| Gray-scale lower and upper bound values	
(a)	0	255
(b)	-812.10^{-5}	1.10^{-5}
(c)	4.10^{-5}	9686.10^{-5}
(d)	1.10^{-5}	42926.10^{-5}

Fig. 4. GAN-based Minkowski maps (b-d) of the image 'Lena' (a) with respect to the luminance criterion $h \equiv f$, using the homogeneity tolerance $m = 40$ in the context of the CLIP mathematical framework. Gray-scale bound values gives the extrema of the Minkowski density functionals values.
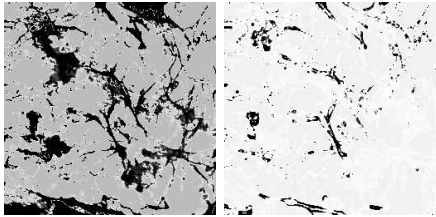
(a) original image f (b) criterion map c

(c) $(\chi_A)_{20}^f$ (d) $(\chi_A)_{20}^c$
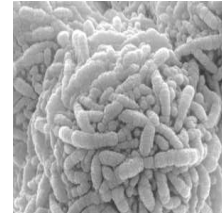
(e) $(P_A)_{20}^f$ (f) $(P_A)_{20}^c$

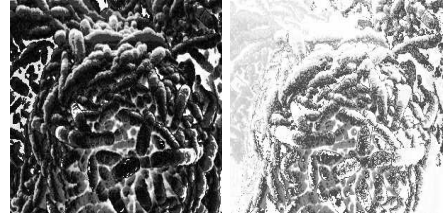(g) $(A_A)_{20}^f$ (h) $(A_A)_{20}^c$

Gray-scale lower and upper bound values		
(a-b)	0	255
(c-d)	-970.10^{-5}	1.10^{-5}
(e-f)	4.10^{-5}	23247.10^{-5}
(g-h)	1.10^{-5}	99213.10^{-5}

Fig. 5. GAN-based Minkowski maps (c-h) of a fibronectin image (a) with respect to the luminance criterion f (c,e,g) and the contrast criterion c (d,f,h), respectively, using the homogeneity tolerance $m = 20$ in the context of the CLIP framework.

(a) original image f

(b) $(\chi_A)_{50}^f$ (c) $(\chi_A)_{50_\triangle}^f$

(d) $(P_A)_{50}^f$ (e) $(P_A)_{50_\triangle}^f$

(f) $(A_A)_{50}^f$ (g) $(A_A)_{50_\triangle}^f$

Gray-scale lower and upper bound values		
(a)	0	255
(b-c)	-656.10^{-5}	1.10^{-5}
(d-e)	4.10^{-5}	13867.10^{-5}
(f-g)	1.10^{-5}	85569.10^{-5}

Fig. 6. GAN-based Minkowski maps (b-g) of a zinc sulfide image (a) with respect to the luminance criterion f, using the homogeneity tolerance $m = 50$ in the context of the CLIP (b,d,f) and LIP (c,e,g) framework, respectively.

5. GAN-BASED MINKOWSKI HISTOGRAMS

The GAN-based Minkowski maps allow to assess the geometrical (area, perimeter) and topological (Euler number) characteristics of the different local image structures. Consequently, the histograms of these maps, named the GAN-based Minkowski histograms, define a topological and geometrical signature of a gray-tone image.

The GAN-based Minkowski histograms provide a statistical distribution of the different GAN-based Minkowski density functionals values of a gray-tone image. They can be defined as the derivative of the cumulative histogram which is an increasing function bounded in $[0, 1]$, as a cumulative distribution function. Thus, the derivative provides the histogram, as a probability density function.

From a 2D gray-tone image f, three GAN-based Minkowski maps are built, and consequently, three histograms providing the distribution of each GAN-based Minkowski density functionals values. These (normalized) histograms, denoted $\mathrm{H}\left(\mu_{m_\bigcirc}^h\right)$ for $\mu \in \{A_A, P_A, \chi_A\}$, are defined by:

$$\mathrm{H}\left(\mu_{m_\bigcirc}^h\right)(t) = \frac{d\mathcal{L}^2\left(\left\{x \in D : \mu_{m_\bigcirc}^h(x) < t\right\}\right)}{\mathcal{L}^2(D)dt} \quad (12)$$

where $d\mathcal{L}^2(X)/dt$ denotes the derivative according to t of the Lebesgue measure $\mathcal{L}^2$ of a subset $X \subseteq D$.

Figure 7 illustrates some GAN-based Minkowski histograms of the image 'Lena' f. The GANs are homogeneous with respect to the luminance criterion $(h \equiv f)$ using the tolerance value $m = 40$ in the context of the CLIP framework.

These GAN-based Minkowski histograms define a topological and geometrical signature of a gray-tone image. They provide a statistical distribution of the topology and geometry of the gray-tone image structures, and not only of the image intensities, like the classical gray-tone histograms. Thanks to this signature, similarity measures between gray-tone images could be determined (distances between histograms). When comparing gray-tone images, the GAN-based Minkowski maps can supply major additional informations: images that cannot be differentiated by their gray-tone histograms (two images visually different can have similar gray-tone histograms) can be differentiated by the histograms of their GAN-based Minkowski histograms. Consequently, application issues to image classification could be adressed, based on this geometrical and topological image characterization.

The next section focuses on the definition of GAN-based Minkowski functions, providing a multiscale analysis of a gray-tone image.

6. MULTISCALE ANALYSIS

When studying the variation of the homogeneity tolerance on the GAN-based Minkowski maps, as it has been done previously for the two others GAN axiomatic criteria, a multiscale analysis of gray-tone images can be performed. This leads to study the impact of a multiscale transformation on these maps. GAN-based Minkowski functions are thus defined.

(a) original image f

(b) $(\chi_A)_{40}^f$ (c) $(P_A)_{40}^f$ (d) $(A_A)_{40}^f$

(e) $\mathrm{H}\left((\chi_A)_{40}^f\right)$ (f) $\mathrm{H}\left((P_A)_{40}^f\right)$ (g) $\mathrm{H}\left((A_A)_{40}^f\right)$

Fig. 7. GAN-based Minkowski maps (b-d) and histograms (e-g) of the image 'Lena' (a) with respect to the luminance criterion $h \equiv f$, using the homogeneity tolerance $m = 40$ in the context of the CLIP framework.

6.1 Impact of the homogeneity tolerance

The GANs are homogeneous regions with respect to an analyzing criterion h using a tolerance $m_\bigcirc$ within a GLIP framework. For one point of the spatial support of a gray-tone image, an increasing family of GANs is obtained with the variation of the homogeneity tolerance $m_\bigcirc$ (Fig. 3). The variation of this parameter allows to built GAN-based Minkowski multiscale maps.

Figure 8 illustrates the GAN-based Minkowski maps and histograms of a brain MR image f with respect to the luminance criterion f using various homogeneity tolerance values: $m = 20$, $m = 30$ and $m = 40$ in the context of the CLIP framework.

These multiscale maps define a GAN-based Minkowski function according to the homogeneity tolerance $m_\bigcirc$. Mathematically, it is thus defined by:

$$\mu_\bigcirc^f(.) : m_\bigcirc \mapsto \mu_{m_\bigcirc}^f(.) \quad (13)$$

Figure 9 shows the cumulative histograms of the GAN-based Minkowski maps according to the homogeneity tolerance $m_\bigcirc$. A 2D representation is obtained where each row is a cumulative histogram. The statistical distribution is given with the use of a color scale.

Figure 10 illustrates these GAN-based Minkowski functions with respect to the luminance criterion, for one point in the brain MR image. This figure shows that in the context of the CLIP framework the function $(A_A)^f(.)$
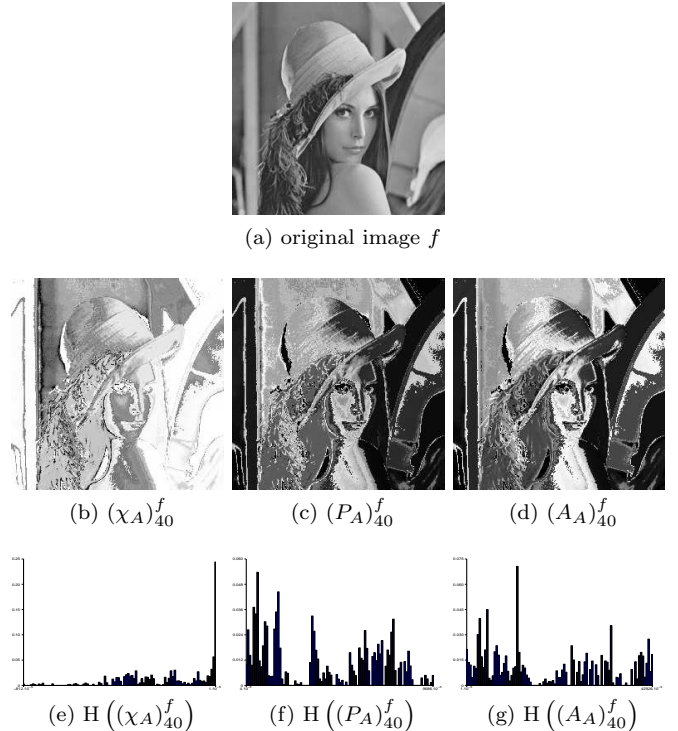
(a) original image f

(b) $(\chi_A)_{20}^f$ (c) $(\chi_A)_{30}^f$ (d) $(\chi_A)_{40}^f$

(e) $(P_A)_{20}^f$ (f) $(P_A)_{30}^f$ (g) $(P_A)_{40}^f$

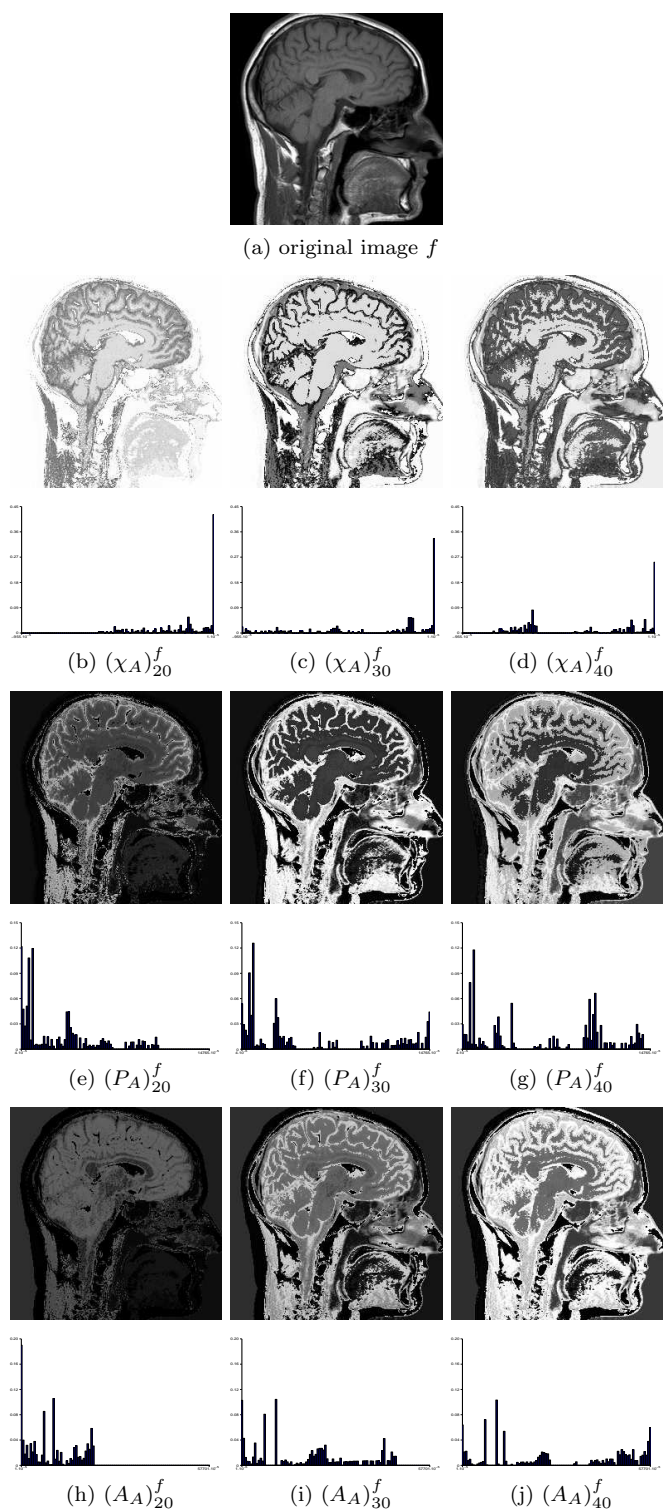(h) $(A_A)_{20}^f$ (i) $(A_A)_{30}^f$ (j) $(A_A)_{40}^f$

Fig. 8. GAN-based Minkowski maps and histograms (b-j) of a brain image (a) with respect to the luminance criterion f, using the homogeneity tolerance values $m = 20$ (b,e,h), $m = 30$ (c,f,i) and $m = 40$ (d,g,j), respectively, in the context of the CLIP framework.
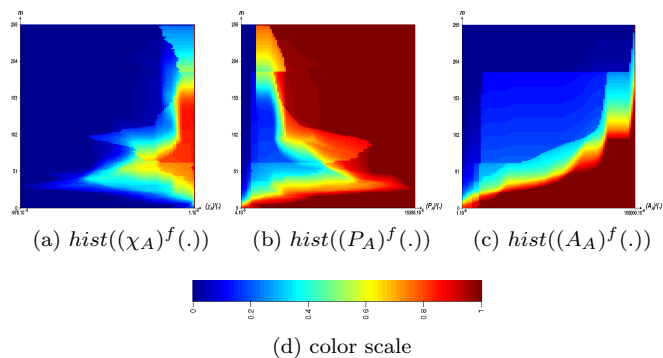

(a) $hist((\chi_A)^f(.))$ (b) $hist((P_A)^f(.))$ (c) $hist((A_A)^f(.))$

(d) color scale

Fig. 9. GAN-based Minkowski cumulative histograms, with respect to the luminance criterion f in the context of the CLIP framework, according to the homogeneity tolerance $m_\bigcirc$ (a-c). A 2D representation is obtained where each row is a cumulative histogram. Abscissa and ordinate coordinates indicate respectively the Minkowski density functionals values and the homogeneity tolerance. The distribution is given with the use of a color scale (d).
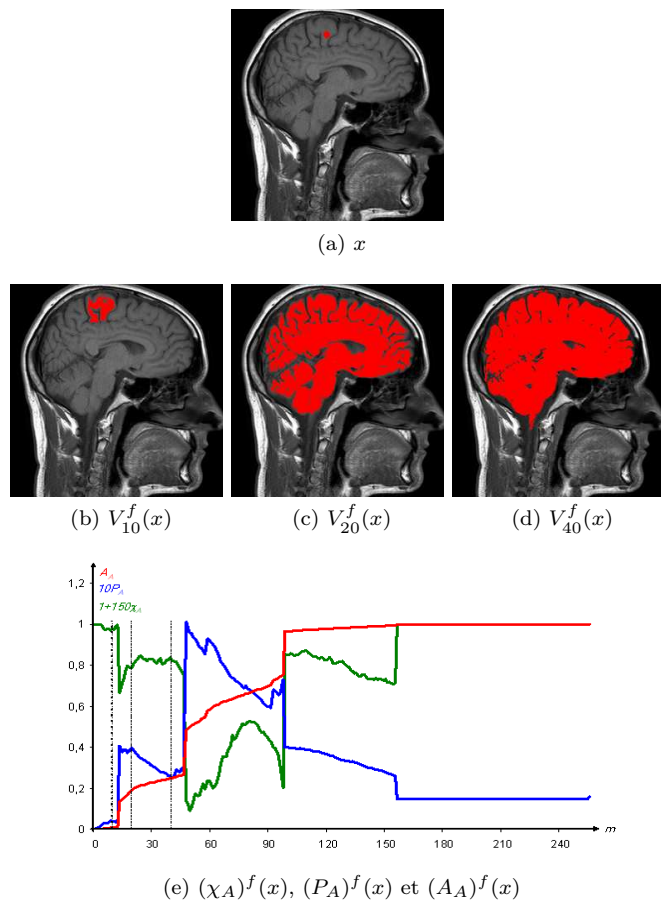

(a) x

(b) $V_{10}^f(x)$ (c) $V_{20}^f(x)$ (d) $V_{40}^f(x)$

(e) $(\chi_A)^f(x)$, $(P_A)^f(x)$ et $(A_A)^f(x)$

Fig. 10. Original image of brain marked with a point x (a), and marked with the GAN of x for the tolerance values $m = 10, 20, 40$ (b-d). Representation of the GAN-based Minkowski functions according to m (e) for this point x. The dot lines represent the results for the Euler number, perimeter, and area of the GAN (b-d) of the point x with $m = 10, 20, 40$.

increases, contrary to $(P_A)^f(.)$ and $(\chi_A)^f(.)$. This property can be generalized to the others GLIP frameworks and criterions: the function $(A_A)^f_{\bigcirc}(.)$ increases, however $(P_A)^f_{\bigcirc}(.)$ and $(\chi_A)^f_{\bigcirc}(.)$ are not monotonous. This is due to the boundary tortuosity and the number of holes that can occur in the GANs. The increasing of $(A_A)^f_{\bigcirc}(.)$ is explained by the increasing of the GANs with respect to $m_{\bigcirc}$ (eq. 6).

Thanks to the variation of the homogeneity tolerance $m_{\bigcirc}$, a GAN-based Minkowski function is defined, providing a multiscale analysis of gray-tone images. The next section is focused on the analysis of the impact of a multiscale transformation on the GAN-based Minkowski maps.

6.2 Impact of a morphological transformation

Mathematical morphology, see Soille (2003), is an important and nowadays a traditional theory in image processing, particularly used for geometrical image analysis. The elementary morphological operators of dilation and erosion (and thus the combined operators of closing and opening) act on image intensities with the use of an operational window named structuring element.

The GAN-based Minkowski maps can be computed on gray-tone images transformed by morphological operators. For instance, figure 11 first illustrates the morphological transforms $T_r(f)$ (T_r denotes the opening (resp. closing) if $r < 0$ (resp. $r > 0$)) using a disk of radius $|r| \in \mathbb{R}_+$ as structuring element of a gray-tone image f of corneal endothelium cells. The GANs $V_m^{T_r(f)}$ are determinated with respect to this transformation $T_r(f)$ using the homogeneity tolerance $m = 20$ in the context of the CLIP framework. Figure 11 shows the associated GAN-based Minkowski maps and histograms.

The variation of the radius r allows to built GAN-based Minkowski multiscale maps. It defines a GAN-based Minkowski function according to the radius r of the structuring element used for the morphological transformation. Mathematically, it is thus defined by:

$$\mu_{m_{\bigcirc}}^{T(f)}(.) : r \mapsto \mu_{m_{\bigcirc}}^{T_r(f)}(.) \tag{14}$$

where r is the radius of the structuring element used for the morphological operator T.

Figure 12 shows the cumulative histograms of the GAN-based Minkowski maps according to the radius r of the structuring element. A 2D representation is obtained where each line is a cumulative histogram. The statistical distribution is given with the use of a color scale.

Figure 13 illustrates these GAN-based Minkowski functions, for one point in the image f of corneal endothelium cells. This figure shows that in the context of the CLIP framework the function $(A_A)_m^{T(f)}(.)$ is not monotonous, contrary to $T(f)(.)$. Thus, whatever the a priori fixed algebraic model and the homogeneity tolerance, the function $\mu_{m_{\bigcirc}}^{T(f)}(.)$ is not monotonous.

A more detailed analysis of the GAN-based Minkowski functions (particularly on the discontinuities of the curves) should allow to obtain shape and/or size informations of the local structures in a gray-tone image, which could be useful for image segmentation and classification.

(a) opening $T_{-4}(f)$ (b) original image f (c) closing $T_4(f)$

(d) $(\chi_A)_{20}^{T_{-4}(f)}$ (e) $(\chi_A)_{20}^{f}$ (f) $(\chi_A)_{20}^{T_4(f)}$

(g) $(P_A)_{20}^{T_{-4}(f)}$ (h) $(P_A)_{20}^{f}$ (i) $(P_A)_{20}^{T_4(f)}$

(j) $(A_A)_{20}^{T_{-4}(f)}$ (k) $(A_A)_{20}^{f}$ (l) $(A_A)_{20}^{T_4(f)}$
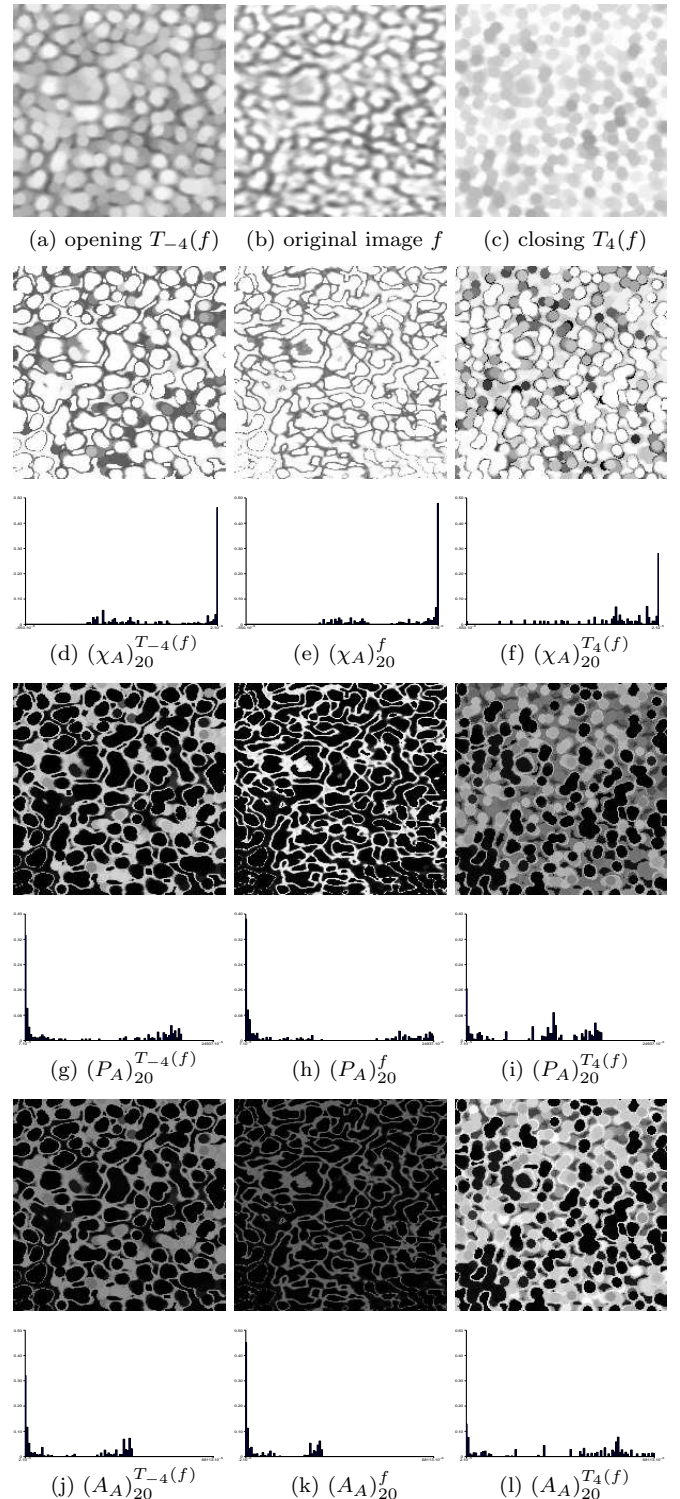
Fig. 11. GAN-based Minkowski maps and histograms (d-l) of an image of corneal endothelium cells (b) with respect to the morphological transformation $T_r(f)$, using the homogeneity tolerance values $m = 20$, in the context of the CLIP framework. T_r denotes the morphological opening ($r < 0$) and closing ($r > 0$) with a disk of radius r.

(a) $hist((\chi_A)_{20}^{T(f)}(.))$ (b) $hist((P_A)_{20}^{T(f)}(.))$ (c) $hist((A_A)_{20}^{T(f)}(.))$
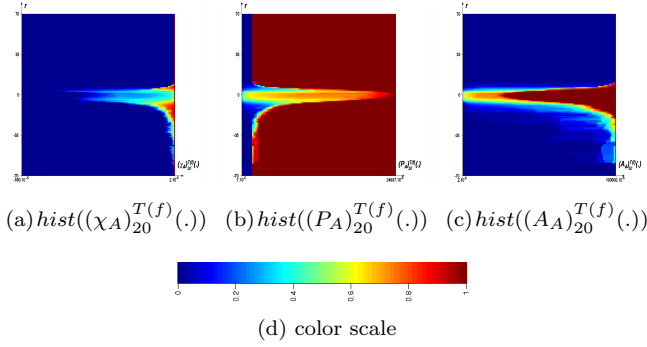

(d) color scale

Fig. 12. GAN-based Minkowski cumulative histograms, with respect to the morphological transformation T_r in the context of the CLIP framework, according to the radius r (a-c). T_r denotes the morphological opening ($r < 0$) and closing ($r > 0$) with a disk of radius r. A 2D representation is obtained where each row is a cumulative histogram. Abscissa and ordinate coordinates indicate respectively the Minkowski density functionals values and the radius. The distribution is given with the use of a color scale (d).
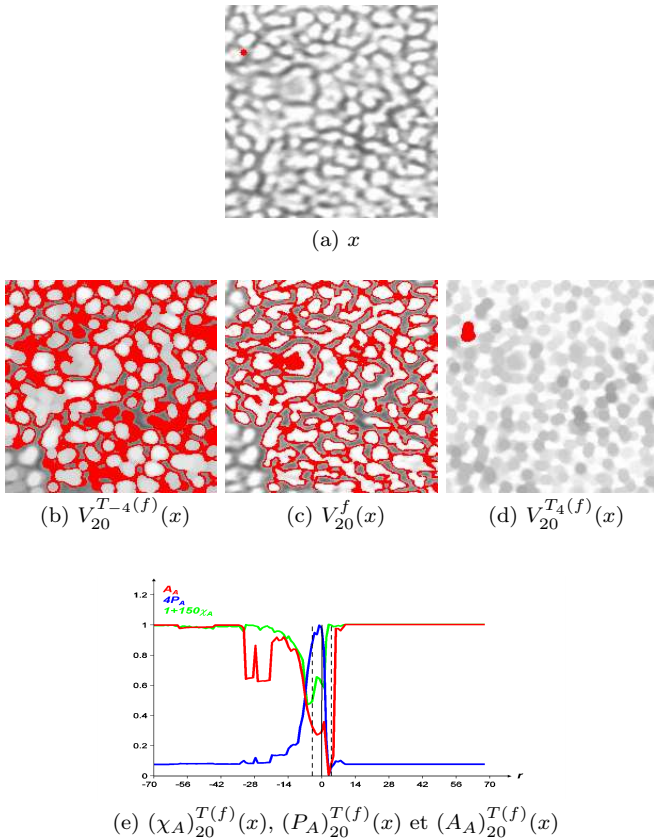

(a) x

(b) $V_{20}^{T_{-4}(f)}(x)$ (c) $V_{20}^{f}(x)$ (d) $V_{20}^{T_4(f)}(x)$

(e) $(\chi_A)_{20}^{T(f)}(x)$, $(P_A)_{20}^{T(f)}(x)$ et $(A_A)_{20}^{T(f)}(x)$

Fig. 13. Original image of cornea cells marked with a point x (a), and marked with the GAN of x for the tolerance value $m = 20$ on transformed images $T_r(f)$ by opening ($r < 0$) and closing ($r > 0$) with disks of radii $r = -4, 0, 4$ (b-d). Representation of the GAN-based Minkowski functions according to r (e) for this point x. The dot lines represent the results for the Minkowski density functionals of the GAN (b-d) of the point x with $r = -4, 0, 4$.

7. CONCLUSION

In this paper, a novel approach for analyzing gray-tone images in a local, adaptive and multiscale way is proposed. Geometrical and topological measurements (Minkowski functionals) are computed on the spatial neighborhood (GAN) of each point of the spatial support of a gray-tone image, enabling to define the so-called GAN-based Minkowski maps by assigning the Minkowski density functional value to each point. The histograms of these maps provide a statistical distribution of the topology and geometry of the gray-tone image structures, and not only of the intensities, like the classical histograms.

The GANs are simultaneously adaptive with the spatial structures, the image intensities and the analyzing scales. They are based on three axiomatic criteria: an analyzing criterion, an algebraic model and an homogeneity tolerance. A visual analysis was performed on the GAN-based Minkowski maps for various analyzing critera and algebraic model. Thanks to the variation of the homogeneity tolerance $m_\bigcirc$, GAN-based Minkowski multiscale maps and histograms are built. These multiscale maps allow to define a GAN-based Minkowski function providing a multiscale analysis of gray-tone images. This leads to look for the impact of a multiscale transformation on these maps, defining an other GAN-based Minkowski function.

Currently, the authors are working on the analysis of the GAN-based Minkowski functions (particularly the discontinuities of the curves) allowing to obtain shape and/or size informations of the structures in a gray-tone image.

ACKNOWLEDGEMENTS

REFERENCES

M. Coster and J.L. Chermant. *Précis d'analyse d'image.* Hermès, 1985.

J. Debayle and J.C. Pinoli. Spatially adaptive morphological image filtering using intrinsic structuring elements. *Image Analysis and Stereology.* **24**:145–158, 2005.

J. Debayle and J.C. Pinoli. General Adaptive Neighborhood Image Processing - Part I: Introduction and theorical aspects. *Journal of Mathematical Imaging and Vision.* **25(2)**:245–266, 2006.

J. Debayle and J.C. Pinoli. General Adaptive Neighborhood Image Processing - PartII: Practical application examples. *Journal of Mathematical Imaging and Vision.* **25(2)**:267–284, 2006.

J. Debayle and J.C. Pinoli. General adaptive neighborhood Choquet image filtering. *Journal of Mathematical Imaging and Vision.* **35(3)**:173–185, 2009.

M. Jourlin and J.C. Pinoli. A Model For Logarithmic Image Processing. *Journal of Microscopy.* **149**:21-35, 1988.

M. Jourlin and J.C. Pinoli. Logarithmic Image Processing, The mathematical and physical framework for the representation and processing of transmitted images.

Advances in Imaging and Electron Physics. **115**:129–196, 2001.

K.R. Mecke and D. Stoyan. *Statistical physics and spatial statistics.* Springer-Verlag Berlin and Heidelberg, New York, 2000.

K. Michielsen and H. De Raedt. Integral-geometry morphological image analysis. *Physics Reports.* **347**:461–538, 2001.

H. Minkowski. Volumen und Oberfläche. *Mathematische Annalen.* **57**:447–95, 1903.

W. Nagel, J. Ohser and K. Pischang. An integral-geometric approach for the Euler-Poincaré characteristic of spatial images. 1999.

A. Oppenheim. Generalized Superposition. *Information and Control.* **11**:528–36, 1967.

J. Osher and F. Mücklich. *Statistical Analysis of Microstructures in Materials Science.* John Wiley and Sons, 2001.

J.C. Pinoli. A General Comparative Study of the Multiplicative Homomorphic, Log-Ratio and Logarithmic Image Processing Approaches. *Signal Processing.* **58**:11–45, 1997.

J.C. Pinoli. The Logarithmic Image Processing model: connections with human brightness perception and contrast estimators. *Journal of Mathematical Imaging and Vision.* **7**:341–358, 1997.

J.C. Pinoli and J. Debayle. Logarithmic Adaptive Neighborhood Image Processing (LANIP): introduction, connections to human brightness perception and application issues. *EURASIP Journal on Advances in Signal Processing.* 2007.

S. Rivollier. *Analyse spectrale morphologique adaptative d'image.* Master's thesis, Ecole Nationale Supérieure des Mines, Saint-Etienne, France, 2006.

S. Rivollier, J. Debayle and J.C. Pinoli. General Adaptive Neighborhood-based Minkowski Maps for Gray-tone Image Analysis. In *Proceedings of ECSIA*, Milan, Italy, 2009.

P. Soille. *Morphological image analysis: principles and applications.* Springer-Verlag, New-York, 1999.

AUTHORS PROFILE

First S. Rivollier. Date of birth: 11/10/1981. Séverine Rivollier received her Master degree in Mathematics in 2006. Since 2006, she is a Ph.D. student in the Image Processing and Pattern Analysis Laboratory within the CIS Center and the LPMG, UMR CNRS 5148 at the 'Ecole Nationale Supérieure des Mines de Saint-Etienne' in France. Her research interests include geometric and morphometric image analysis through the general adaptive neighborhoods.

Second J. Debayle. Date of birth: 20/12/1977. Johan Debayle received his Ph.D. degree in the field of image processing and analysis in 2005. In the beginning of 2006, he joined the French National Institute for Research in Computer Science and Control (INRIA) as a postdoctoral fellow in the field of biomedical image analysis. Since 2007, he is assistant professor in the Image Processing and Pattern Analysis Laboratory within the CIS Center and the LPMG, UMR CNRS 5148 at the 'Ecole Nationale Supérieure des Mines de Saint-Etienne' in France. His research interests include adaptive image processing and morphological image analysis.

Third J.C. Pinoli. Date of birth: 27/08/1959. Jean-Charles Pinoli received Master, Doctorate of Science and 'Habilitation à Diriger des Recherches' degrees in Applied Mathematics in 1983, 1987 and 1992, respectively. From 1985 to 1989, he was member of the opto-electronics department of the Angenieux (Thales) company, Saint-Héand, France, where he pioneered researches in the field of digital imaging and artificial vision. In 1990, he joined the Corporate Research Center of Pechiney Company, Voreppe, France, and was member of the computational technologies department in charge of the imaging activities. Since 2001, he is full professor at the 'Ecole Nationale Supérieure des Mines de Saint-Etienne'. He leads the Image Processing and Pattern Analysis Laboratory within the CIS Center and the LPMG, UMR CNRS 5148. His research interests and teaching include Image Processing, Image analysis, Mathematical Morphology and Computer Vision.